

An improved heat pulse method to measure low and reverse rates of sap flow in woody plants[†]

STEPHEN S. O. BURGESS,^{1,5} MARK A. ADAMS,¹ NEIL C. TURNER,² CRAIG R. BEVERLY,³ CHIN K. ONG,⁴ AHMED A. H. KHAN⁴ and TIM M. BLEBY¹

¹ Department of Botany, University of Western Australia, Nedlands, WA, 6907, Australia

² CSIRO Plant Industry, Private Bag No. 5, Wembley, WA 6913, Australia

³ Agriculture Victoria, DNRE Chiltern Valley Road, Rutherglen, VIC, 3685, Australia

⁴ International Centre for Research in Agroforestry (ICRAF), PO Box 30677, Nairobi, Kenya

⁵ Present address: Department of Integrative Biology, University of California, Berkeley, CA, 94720-3140, USA

Received May 26, 2000

Summary The compensation heat pulse method (CHPM) is of limited value for measuring low rates of sap flow in woody plants. Recent application of the CHPM to woody roots has further illustrated some of the constraints of this technique. Here we present an improved heat pulse method, termed the heat ratio method (HRM), to measure low and reverse rates of sap flow in woody plants. The HRM has several important advantages over the CHPM, including improved measurement range and resolution, protocols to correct for physical and thermal errors in sensor deployment, and a simple linear function to describe wound effects. We describe the theory and methodological protocols of the HRM, provide wound correction coefficients, and validate the reliability and accuracy of the technique against gravimetric measurements of transpiration.

Keywords: compensation method, heat pulse velocity, reverse flow, transpiration, water transport, water use, woody roots.

Introduction

Measurements of sap flow in xylem tissue based on conduction and convection of heat are widely employed to investigate water relations of plants. Thermometric methods of estimating sap flow are easily automated (Smith and Allen 1996), and only moderately invasive (Marshall 1958).

Thermometric techniques include three broad categories; those that trace the movement of a short pulse of heat in the sap stream, those that measure heat transported away from a controlled heat source by moving sap and those that relate heat dissipation to sap flow by an empirical relationship. There are numerous variants within the first two categories and the suitability of each technique to specific applications differs according to their respective capabilities and constraints (Swanson 1994, Smith and Allen 1996).

Methods that utilize a heat pulse are often favored because of their simple instrumentation and low power requirements. Of the heat pulse techniques, the compensation heat pulse

method (CHPM) has been most widely used (Edwards et al. 1996). A solid theoretical basis for converting heat pulse velocities (V_h) measured by CHPM to quantitative rates of sap flow in plants was developed several decades ago (reviewed by Swanson 1994). Much research in forestry (e.g., Dunn and Connor 1993, Dye and Olbrich 1993, Barker and Becker 1995, Hatton et al. 1995, Becker 1996, Dye et al. 1996, Fenyvesi et al. 1998), hydrology (e.g., Salama et al. 1994, Dawson 1996, Vertessy et al. 1997), horticulture (e.g., Renquist et al. 1994, Green and Clothier 1995, Moreno et al. 1996, Green et al. 1997) and basic plant physiology (e.g., McAneney et al. 1992, Dye 1996, Zotz et al. 1997) has relied on CHPM.

The limitations of CHPM for measuring low rates of flow have recently been highlighted (Becker 1998). The CHPM requires a heater to be inserted in the xylem a fixed distance (commonly 0.25 cm) upstream from the midpoint between two temperature sensors. The velocity of the heat pulse is determined by recording the time it takes for the pulse to travel by convection to the midpoint between temperature sensors, at which time the sensors record the same temperature. When sap flow rates are low, the heat pulse may dissipate by conduction before it reaches the measurement point. In such cases, the sensors record equal temperatures, because the temperatures have returned to initial values. For this reason, low, zero and reverse rates of flow are overestimated. Furthermore, overestimation of near zero velocities is exacerbated by wound correction functions, which as derived by Swanson and Whitfield (1981), do not pass through the origin.

Lower limits to measurement depend on the sensitivity of temperature sensors and rates of thermal diffusivity in xylem. Consequently, published measurement thresholds vary substantially. Based on standard commercial CHPM equipment, Becker (1998) estimated that sap velocities (V_s , which are generally comparable in magnitude to V_h ; see below) between 3.6 and 7.2 cm h⁻¹ (0.01–0.02 mm s⁻¹) are indistinguishable from zero. Studies with custom-built devices have suggested similarly small thresholds for V_h , e.g., 4 cm h⁻¹ by Burgess et

[†] Equations 4, 7, 8 and 10 have been revised in accordance with the corrections published in *Tree Physiology*, Volume 21, Issue 15, page 1157.

al. (1998) and 3 cm h^{-1} by Swanson and Whitfield (1981), although Barrett et al. (1995) reported a much higher threshold of $9.4\text{--}15.7 \text{ cm h}^{-1}$. Very small thresholds have been achieved by using modified sensor spacings. Lassoie et al. (1977) placed the heater 0.15-cm upstream of the midpoint between temperature sensors and achieved a V_h threshold of 1.8 cm h^{-1} . However, with reduced spacing, errors in the positioning of sensors have an increased impact on measurement accuracy.

A significant fraction of the range of V_h measured in most trees falls below the measurement threshold. For example, Swanson (1983) cited a V_h range of $0\text{--}35 \text{ cm h}^{-1}$ for conifers and $0\text{--}30 \text{ cm h}^{-1}$ for diffuse porous hardwoods, with most measurements being below 20 cm h^{-1} . Dunn and Connor (1993) reported a daily mean V_h of $10\text{--}12 \text{ cm h}^{-1}$ for mountain ash (*Eucalyptus regnans* F. Muell.). For the 35 species for which Wullschlegel et al. (1998) listed basal area versus daily water use, mean V_s is $16.6 \text{ cm}^3 \text{ cm}^{-2} \text{ h}^{-1}$. Although sap flows quickly in some species such as kiwifruit (*Actinidia deliciosa* (A. Chev.) C. F. Liang et A. R. Ferguson) (Green and Clothier 1988), it appears that peak V_h in most woody species is seldom greater than $35\text{--}45 \text{ cm h}^{-1}$, with mean rates less than half this value. Consequently, an inability with the CHPM to measure V_h below 3 or 4 cm h^{-1} will affect the lower $10\text{--}30\%$ of measurements (see also Burgess et al. 2000b). Measurements of transpiration during winter, at night (Benyon 1999) or by understory species are likely to be most affected.

The CHPM and several other thermometric methods have also been used in root studies of seasonal water acquisition (Burgess et al. 1998), competition for water by agroforestry species (Lott et al. 1996, Smith et al. 1999) and the fate of irrigation water applied to plants (Cabibel and Do 1991, Green et al. 1997). In roots, xylem sap flow can be either acropetal or basipetal (e.g., when water is being redistributed within the soil (Burgess et al. 1998)). Clearly, thermometric methods that fail under conditions of reverse flow (e.g., the CHPM) or cannot detect the direction of flow (e.g., some heat balance and thermal dissipation methods) will result in incomplete or erroneous findings (Burgess et al. 2000a). We sought to develop an improved heat-pulse-based technique (the heat ratio method, HRM) that would be sensitive to the direction of sap flow and able to measure low rates of flow accurately.

Theory

Measurement and calculation of heat pulse velocity

CHPM The theory of operation of the CHPM has been described elsewhere (e.g., Swanson and Whitfield 1981, Smith and Allen 1996) and is only briefly reviewed here for comparison with the HRM.

For the CHPM, two probes containing temperature sensors are aligned with the axis of a plant stem or root and inserted radially to equal depths in the xylem. A heater element is similarly inserted at a fixed distance upstream from the midpoint between the temperature probes. A common configuration locates the heater 0.5 cm from the upstream temperature probe and 1.0 cm from the downstream probe (here denoted as a

$-0.5, 0, 1.0 \text{ cm}$ configuration). During measurement, wood and sap are heated in pulses and convection through the flowing sap stream carries the heat toward the midpoint between the temperature probes. When both temperature probes have warmed to the same degree, the heat pulse has moved the 0.25 cm from the heater, i.e., to the midpoint between the probes. The time taken for the heat pulse to move this distance is used to calculate heat pulse velocity (V_h):

$$V_h = \frac{x_1 + x_2}{2t_0} 3600, \quad (1)$$

where t_0 is time to thermal equilibration of the downstream and upstream probes after release of the heat pulse, and x_1 and x_2 denote distances (cm) between the heater and the downstream and upstream temperature probes, respectively (we use these terms as they apply in the case when water flows from soil to leaves). A negative value is assigned to x_2 because it is located on the opposite side of the heater to x_1 .

HRM The heat ratio method (HRM) measures the ratio of the increase in temperature, following the release of a pulse of heat, at points *equidistant* downstream and upstream from a line heater. Heat pulse velocity is calculated as (Marshall 1958):

$$V_h = \frac{k}{x} \ln(v_1/v_2) 3600, \quad (2)$$

where k is thermal diffusivity of green (fresh) wood, x is distance (cm) between the heater and either temperature probe, and v_1 and v_2 are increases in temperature (from initial temperatures) at equidistant points downstream and upstream, respectively, $x \text{ cm}$ from the heater. The probe positions relative to the heater used with the HRM are -0.6 and 0.6 cm , hence $x = 0.6 \text{ cm}$. Thermal diffusivity (k) is assigned a nominal value of $2.5 \times 10^{-3} \text{ cm}^2 \text{ s}^{-1}$ (Marshall 1958) and this value is further resolved once sapwood properties have been measured (see below).

Influence of measurement time

Marshall (1958) stated that the v_1/v_2 ratio remains constant with time, rendering the time of measurement unimportant; however, Marshall's (1958) description did not account for departures from the ideal state that can arise from two sources. First, patterns of heat transfer are altered by blocking of, and damage to, xylem vessels caused by insertion of probes. Additional disruption of heat transfer occurs because the thermal properties of the sensor material (e.g., stainless steel) differ from those of xylem. Second, even with careful probe placement, it is likely that probe spacing will be at least slightly asymmetrical. Both of these departures from the ideal cause v_1/v_2 to change with time with the result that measurement time affects results. Ratios of v_1/v_2 will approach an ideal value asymptotically, with the rate of change decaying exponentially with time following the heat pulse (Figure 1). However, even in the most extreme cases, the rate of change in v_1/v_2 after

60 s becomes extremely small and ratios will be effectively linear and have a slope of less than 0.01 (Figure 1). This finding has two important implications. First, measurements should be made at least 60 s after the heat pulse has been released. Second, multiple sampling of v_1/v_2 is possible. For example, because our multiplexer cycle speed was 2.8 s, we logged and averaged 14 measurements of v_1/v_2 over the period 60–100 s to minimize the contribution of any random signal noise to measurements. Because v_1/v_2 is effectively linear between 60 and 100 s, the value of these averaged ratios will differ from an “ideal” value measured at the median time of 80 s by < 0.4% for extreme cases, although generally this difference will be negligible. Because random variation in v_1/v_2 arising from thermal and electronic interference can contribute an error an order of magnitude greater, multiple sampling of v_1/v_2 is desirable.

Correction for probe misalignment

All heat pulse velocity techniques are highly sensitive to errors arising from inaccurate probe spacing. For example, when the CHPM is configured as described earlier, a 1-mm error in spacing for either probe will introduce a 20% error in calculations of V_h . With the CHPM, probe misplacement is assessed by placing over-length probes in drill holes and measuring the spacing and angle of the protruding probes (Hatton et al. 1995). With the HRM, probe placement is measured *in situ*, which takes into account thermal as well as physical symmetry (e.g., whether thermocouples or thermistors lie symmetrically within the probe housing (Becker 1998)). At $V_h = 0$ (which can be imposed by severing the root or stem), probe spacing is calculated as:

$$x_2 = \sqrt{(4kt \ln(v_1/v_2) + x_1^2)}, \quad (3)$$

where x_2 denotes the incorrectly spaced probe, x_1 is assumed to be correctly spaced at 0.6 cm and t is measurement time

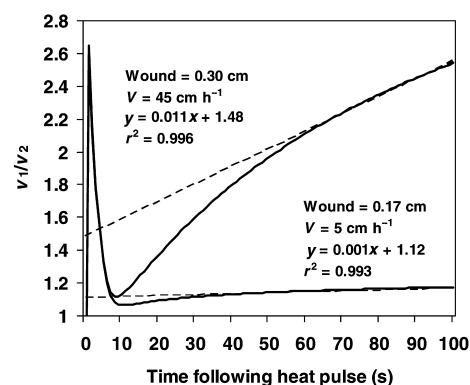


Figure 1. Modeled changes in v_1/v_2 ratios with time for a small wound width (0.17 cm) and low sap velocity (5 cm h^{-1}) compared with a large wound width (0.30 cm) and high sap velocity (45 cm h^{-1}). Note that, with both mild and extreme departures from the ideal caused by sensor implantation, v_1/v_2 is essentially linear between 60 and 100 s as indicated by the r^2 values for the linear regressions fit over the data for this period.

(Equation 1). Because time has an essentially linear effect on Equation 3 over 60–100 s, it can be solved by using the median measurement time (80 s) or by averaging solutions calculated for each t value used in the measurement series. Results of the two approaches differ by < 1% in extreme cases.

Once calculated, x_1 and x_2 values can be derived with Equation 3, and corrected V_h calculated as (adapted from Marshall 1958):

$$V_h = \frac{4kt \ln(v_1/v_2) - (x_2^2) + (x_1^2)}{2t(x_1 - x_2)} 3600. \quad (4)$$

By correcting a small sample of data and comparing uncorrected values with corrected values, a simple linear relationship can be derived that can be used to correct the remaining data.

Because it is not known which probe is incorrectly positioned, our approach was to also solve Equations 3 and 4 assuming x_1 is incorrectly positioned and then average the two solutions to yield an intermediate solution (Burgess et al. 1998). Use of this intermediate solution prevents biasing corrections of sap flow in either direction. Results for the two extreme scenarios differ from the intermediate solution by ± 4 to 22% for moderate (0.05 cm) to extreme (0.3 cm) positioning errors, respectively (see Figure 2B), indicating that large errors in probe placement cannot be corrected with sufficient certainty and these cases should probably be abandoned. Examples of the effects of a large spacing error on measurements, the correction procedure and its results are shown in Figures 2A and 2B.

Correction for wounding

Installing sensors in xylem tissue causes substantial mechanical damage. In addition to the interruption of flow pathways

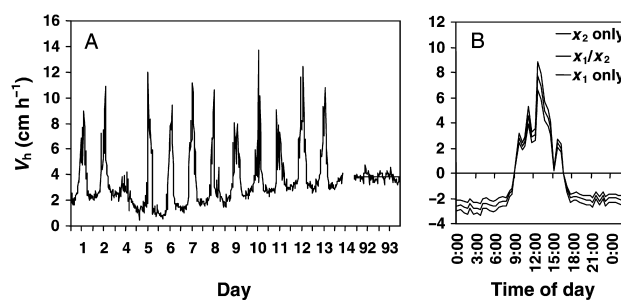


Figure 2. (A) Example of an episode of reverse flow (hourly means) in a lateral root of *Eucalyptus camaldulensis* Dehnh. erroneously measured by probes with a large spacing error ($\sim 0.2 \text{ cm}$). Data on Days 92 and 93 were collected after the root was severed to stop flow and indicate the potential for ambient temperature fluctuations to disturb measurements in uninsulated sensors. The straight line shows the mean erroneous velocity arising from a probe spacing error. (B) Example of corrected data (corresponding to Day 7 in Figure 2A) derived with the protocols described in the text. The middle series is the intermediate solution, which assumes both downstream and upstream probes contributed to the spacing error, whereas the other two series assume that only probe x_1 or x_2 was incorrectly spaced.

by the insertion of the probes, intact vessels may become occluded as the plant responds to wounding by forming tyloses (Barrett et al. 1995). The resulting region of nonconducting wood around the site of probe insertion affects measurement of V_h by decreasing v_1/v_2 . Swanson and Whitfield (1981) used a finite-difference numerical model to produce a simple algebraic equation for wound correction. The model calculates three coefficients (a , b and c , for varying wound widths) to calculate corrected heat pulse velocity (V_c) measured with the CHPM according to:

$$V_c = a + bV_h + cV_h^2. \quad (5)$$

Swanson (1983) also generated a limited number of coefficients for symmetric probe configurations such as the HRM. Unfortunately, as with the coefficients for the CHPM, Swanson's (1983) solutions do not pass through the origin and the resulting corrections yield a poor approximation of low, zero and reverse rates of sap flow. We therefore developed a new numerical model to supply appropriate wound correction coefficients. To correct heat pulse velocity measured with the HRM, three coefficients, b , c and d are used in Equation 6:

$$V_c = bV_h + cV_h^2 + dV_h^3. \quad (6)$$

Determining sap velocity

Only a portion of xylem tissue (the xylem lumen) contains moving sap. Heat pulse probes effectively measure a weighted average of the velocities of moving sap and "stationary" wood (Marshall 1958). Sap velocity can be determined on an areal basis by measuring the fractions of sap and wood in xylem and accounting for their differing densities and specific heat capacities. Barrett et al. (1995) modified Marshall's (1958) equation relating V_c to sap velocity (V_s) as:

$$V_s = \frac{V_c \rho_b (c_w + m_c c_s)}{\rho_s c_s}, \quad (7)$$

where ρ_b is the basic density of wood (dry weight/green volume), c_w and c_s are specific heat capacity of the wood matrix (1200 J kg⁻¹ °C⁻¹ at 20 °C (Becker and Edwards 1999)) and sap (water, 4182 J kg⁻¹ °C⁻¹ at 20 °C (Lide 1992)), respectively, m_c is water content of sapwood and ρ_s is the density of water.

Converting sap velocity to sap flow

Volumetric flow can readily be derived as the product of sap velocity (V_s) and cross-sectional area of conducting sapwood. Gross wood cross-sectional area is calculated from its under-bark radius. Heartwood area is discounted by staining the sapwood (Goldstein et al. 1998) or by observing the dark color often associated with heartwood. Where sap velocity is estimated at several radial depths, total sapwood area is divided into concentric annuli delimited by the midpoints between measurement depths. In this way, point estimates of sap velocity are weighted according to the amount of conducting sap-

wood in the annulus they sample.

Materials and methods

Measurement protocol

Thermocouple temperature probes were constructed by placing two or three fine-gauge (36 AWG) copper-constantan thermocouple junctions inside a stainless steel 18-gauge syringe needle (1.3 mm in diameter and 30 mm in length). Junctions were insulated with Teflon tape before positioning them 5, 15 or 25 mm from the needle tip. The needle tip was sealed with solder and the needle base filled with epoxy resin to secure and waterproof the contents of the probe. Individual thermocouple circuits were connected to a 64-channel multiplexer (Model AM32 or AM416, Campbell Scientific Inc., Logan, UT), which in turn was connected to a data logger (Model 21X, Campbell Scientific Inc.).

Line heater elements were formed by tightly coiling ~20 cm of nichrome wire (36 AWG, 79 Ω m⁻¹) and insulating the coil before inserting it in a 30-mm long syringe needle. The resulting ~16-Ω heaters were connected in parallel to a 12-V lead acid battery by a relay that allowed a controlled pulse of heat (usually 3 s duration) to be released at regular intervals. A 12-W solar panel was used to maintain battery voltage in the field. (An earlier 38-Ω heater design, which necessitated a 6-s heat pulse, was used for some experiments. Side by side comparisons suggested that the 16- and 38-Ω heaters gave similar results (see also Swanson and Whitfield 1981).)

Probes were inserted in trees by first drilling 1.3-mm diameter holes 30 mm deep into xylem tissue. A steel drilling guide was strapped to the tree to ensure holes were drilled parallel at fixed spacings along the plant stem-root axis. Petroleum jelly was used to ease probe insertion and maintain thermal contact between the probe and wood tissue (Barrett et al. 1995).

CHPM configuration Temperature probes were placed 0.7-cm upstream and 1.2-cm downstream from the heater (a -0.7, 0, 1.2 cm configuration). This arrangement, which is wider than the commonly used -0.5, 0, 1.0 cm configuration (Green and Clothier 1988, Swanson 1994, Hatton et al. 1995), was adopted because the base width of the hypodermic needles (0.6 cm) was too large to allow the smaller spacing. The configuration is similar to standard spacings in that the heater is located 0.25 cm downstream from the midpoint between temperature sensors. Although the wound correction coefficients developed by Swanson and Whitfield (1981) apply generally to our configuration, we generated new coefficients specific to our configuration based on the model described below.

Measurements of V_h were made every 30 min. Temperatures of individual probes were first measured by taking an average over a period of approximately 10 s. A pulse of heat was then released into the xylem and subsequent probe temperatures were measured every 1 s for 300 s, by which time the heat pulse had dissipated. At 1-s intervals, initial probe temperatures were subtracted from current temperatures so that only

the relative temperature change was recorded for each thermocouple. Relative temperature change in downstream probes was compared with that in the corresponding upstream probes. When the downstream temperature increase was equal to or greater than the upstream temperature increase, time (t_0) was recorded. To allow time for the probe temperatures to change from their initial equilibrium at ambient temperature in the xylem, comparisons were not made until 15 s after the release of the heat pulse (cf. Green and Clothier 1988).

HRM configuration Temperature probes were placed equidistant to the heater with a spacing of $-0.6, 0, 0.6$ cm. Temperature increases were measured as with the CHPM and v_1/v_2 ratios were logged between 60 and 100 s after the release of the heat pulse and the calculations were then averaged.

Calculation of thermal diffusivity

Thermal diffusivity (k) was initially taken as $2.5 \times 10^{-3} \text{ cm}^2 \text{ s}^{-1}$ ($2.5 \times 10^{-7} \text{ m}^2 \text{ s}^{-1}$) and two methods (simultaneous solution and empirical measurement) were tested to measure actual k .

Simultaneous solution This method was based on the reasoning of Cohen et al. (1993) who used the CHPM (which is independent of k) to calculate V_h alongside the t_{\max} method (which requires k , see Cohen et al. 1993 for details) and then solved the two equations simultaneously to estimate k . In our case, we compared measurements of V_h made with the CHPM and HRM in the stem of a single *Banksia prionotes* Lindley tree (see Burgess et al. 2000b). Values of V_h within the common range of both techniques were compared over a 10-day measurement period during April and June 1998.

Empirical measurement For the empirical measurement, we calculated k ($\text{cm}^2 \text{ s}^{-1}$) from Equation 8 (Marshall 1958):

$$k = \frac{K_{\text{gw}}}{\rho c} 10000, \quad (8)$$

where K_{gw} is thermal conductivity, ρ is density (kg m^{-3}) and c is specific heat capacity of green (fresh) wood.

The value of K_{gw} was first calculated according to Equation 9 modified from Swanson (1983):

$$K_{\text{gw}} = K_s m_c \frac{\rho_b}{\rho_s} + K_w (1 - m_c \frac{\rho_b}{\rho_s}), \quad (9)$$

where K_s is thermal conductivity of water ($5.984 \times 10^{-1} \text{ J m}^{-1} \text{ s}^{-1} \text{ }^\circ\text{C}^{-1}$ at 20°C (Lide 1992)) and K_w is thermal conductivity of dry wood matrix. We calculated K_w as (Equation 10, Swanson 1983):

$$K_w = 0.04182(21.0 - 20.0 F_v), \quad (10)$$

where F_v is the void fraction of wood defined as (cf. Swanson 1983):

$$F_v = 1 - \left(\frac{\rho_b 0.6536 + m_c}{1000} \right). \quad (11)$$

Specific heat capacity of green wood was calculated according to its constituent parts (modified from Edwards and Warwick 1984):

$$c = \left(\frac{w_d c_w + c_s (w_f - w_d)}{w_f} \right), \quad (12)$$

where w_f is fresh weight and w_d is oven-dried weight of the sample (kg).

Water content and density of the sapwood were measured on wood cores taken from the stem during April and June.

Correction for wounding

We used a two-dimensional finite element model (Beverly, Burgess and Bleby; unpublished data) based on the formulation presented by Swanson and Whitfield (1981). The model supports linear and quadratic triangular isoparametric elements and solves for temperature at both temperature sensors under conditions of uniform sap velocity using an equation based on conservation of energy and continuity. Both the temperature dependent (Dunlap 1912) and temperature invariant (Swanson and Whitfield 1981) versions of wood-sap mixture density functions are used as constitutive equations. The temporal derivative is reduced based on a time-weighted Picard scheme and the assembled matrix is solved by means of a frontal solver. Probe spacings, wound and probe diameters and material characteristics are all user defined. Based on this information, the program generates the corresponding finite element mesh by means of an adaptive gridding algorithm to ensure maximum grid refinement occurs in those zones adjacent to the heater and sensor probes.

The developed model enabled the analysis of any host/heater/sensor material arranged in any spatial configuration and accommodates any probe diameter and wound width. We analyzed the effect of wounding on V_h measured by the HRM based on results derived from the finite element model that was configured to calculate the correction coefficients for two symmetrically spaced sensors (-0.6 cm, 0 , 0.6 cm and -0.5 cm, 0 , 0.5 cm). Coefficients b , c and d were then used to correct heat pulse velocity based on the polynomial function in Equation 6.

The accuracy of the polynomial solution incorporating coefficients b , c and d was compared with a linear solution with a fourth coefficient, B :

$$V_c = B V_h. \quad (13)$$

Wound widths were estimated by drawing dye through sections of xylem to identify nonconductive vessels (after Goldstein et al. 1998).

Sensitivity to temperature fluctuations

Potential effects of temperature fluctuations on HRM mea-

measurements were investigated in two ways. First, uninsulated roots containing HRM sensors were severed and placed on the soil surface. We continued to measure rates of flow in the root to check if deviations from zero might represent errors arising from radiant heat inputs or losses (e.g., from direct sunlight or diurnal variation in air and soil temperatures). In a second investigation, we stopped the pulsing of heat while continuing measurements of probe temperatures. In this way we sought to exaggerate the relative importance of external temperature changes on the measurement system.

Sensitivity to probe spacing

We measured V_h with several probe configurations to test whether this parameter affects the quality of the results. Symmetric spacings tested were 1.2, 0.75, 0.6 and 0.5 cm.

Validation

Because of the difficulty of inducing known rates of reverse flow in plants, tests were made when sap flow was positive. These tests relate equally to the performance of the HRM under conditions of reverse flow, because the symmetrically configured HRM behaves identically under either direction of flow.

A potted 8-year-old *Eucalyptus marginata* J. Donn ex Sm. tree was placed on a digital recording balance in a greenhouse. The exposed soil surface was covered with plastic sheeting to minimize evaporation from the soil. Two sets of HRM probes were installed on the stem of the tree. For each set, sap velocity was sampled at radial depths of 0.5 and 1.5 cm from the outer edge of the sapwood. Measurements were combined according to the cross-sectional area of xylem in the stem at each depth sampled by the thermocouple junctions. Consequently, sap velocities measured with the outermost junction were multiplied by the cross-sectional area of the outer 1-cm annulus of sapwood, whereas values for the deeper junction were multiplied by the remaining area of sapwood (an annulus about 1.7 cm wide). Total sapwood area of the stem was 29.8 cm².

Weight loss measured with the balance and sap flow measured with the HRM were recorded every 10 min over a period of several days. The amount of water lost was averaged for each 0.5-h period and converted to flow rate (cm³ h⁻¹) for comparison with measured sap flow. The potted tree was watered periodically.

At the end of the experiment, the tree trunk was severed, recut under water ~15 cm from the cut end, and the freshly cut end placed in a solution of basic fuchsin dye. After transpiring for several hours, the tree was removed from the dye solution, the wood sectioned and patterns of dye staining observed to determine the location of conductive sapwood and the width of wounds around sites of probe insertion.

The experiment was repeated with a set of probes with a modified spacing (–0.5, 0, 0.5 cm) installed in a similar-sized *E. marginata* tree (sapwood area = 32.8 cm²).

Results

Determining thermal diffusivity

The simultaneous solution method and the empirical method yielded similar values of k . The simultaneous solution method gave k values that were within the expected range of 1.4×10^{-3} to 4.0×10^{-3} cm² s⁻¹, which are the values for water and dry wood, respectively (Marshall 1958). For *B. prionotes*, values were $2.30 \pm 0.03 \times 10^{-3}$ cm² s⁻¹ ($n = 392$) and $2.33 \pm 0.04 \times 10^{-3}$ cm² s⁻¹ ($n = 296$) for April and May–June, respectively. The empirical method gave k values for the *B. prionotes* stem of $2.33 \pm 0.01 \times 10^{-3}$ cm² s⁻¹ ($n = 5$) in April and $2.26 \pm 0.05 \times 10^{-3}$ cm² s⁻¹ ($n = 2$) in June.

Correction for wounding

Table 1A lists the wound correction coefficients (b , c , d and B) calculated with the numerical model for a –0.6, 0, 0.6 cm probe configuration, 1.3-mm diameter stainless steel probes and a measurement time of $t = 60$ – 100 s. Additional coefficients for a –0.5, 0, 0.5 cm configuration are shown in Table 1B. Figure 3 compares the polynomial and linear solutions for a 0.20-cm wound.

Sensitivity to temperature fluctuations

External temperature changes caused V_h measured by HRM to fluctuate 0.5–1 cm h⁻¹ in the severed root (cf. Days 92 and 93 in Figure 2A). In general, thermocouple pairs close to the root surface were more affected by external temperature changes than thermocouple pairs located deeper in the root (data not shown).

There was a large fluctuation in V_h when the influence of external temperature changes was exaggerated by stopping the pulsing of heat, the apparent result of small but unequal changes in probe temperature creating large v_1/v_2 ratios (see Equation 2). A comparison of data obtained with normal heater operation and with the heater disabled showed poor correlation ($r^2 = -0.0013$), suggesting these effects were random.

Sensitivity to spacing

Of the four spacings tested, 1.2-cm showed the most unexplained variation. For example, data obtained at the 1.2-cm spacing were more weakly correlated with both total solar radiation ($r^2 = 0.77$) and V_h as measured by the CHPM ($r^2 = 0.75$) than data obtained at the standard 0.6-cm spacing ($r^2 = 0.88$ and 0.87).

Validation

Resolution of the balance (± 20 g) was sufficiently sensitive to allow comparisons with the relatively low rates of flow measured by the HRM during the cold, generally overcast conditions that prevailed during the experiment. The effective resolution of the balance was 40 cm³ h⁻¹, which is equivalent to a sap velocity of about 1.2 cm³ cm⁻² h⁻¹ in the trees.

For both trees, measurements made with the HRM were closely correlated with gravimetric measurements. Quantities of water flowing through the stem at night tended to be slightly

Table 1. (A) Correction coefficients for numerical solutions derived for a range of wound diameters and corresponding to a $-0.6, 0, 0.6$ cm probe configuration, where the stainless steel probes are 1.3 mm in diameter. Solutions were derived based on modeled temperature data at $t = 60\text{--}100$ s. Coefficients b , c and d apply to Equation 6. Coefficient B is a linear approximation (Equation 13) of the polynomial relationship described by Equation 6. (B) Additional coefficients generated for a $-0.5, 0, 0.5$ cm probe configuration, with 1.3-mm diameter stainless steel probes.

| Wound (cm) | b | c | d | r^2 | B | r^2 |
|---|--------|---------|--------|--------|--------|--------|
| A. $-0.6, 0, 0.6$ -cm probe configuration | | | | | | |
| 0.17 | 1.6565 | -0.0014 | 0.0002 | 1.0000 | 1.7023 | 0.9993 |
| 0.18 | 1.7077 | -0.0014 | 0.0002 | 1.0000 | 1.7585 | 0.9992 |
| 0.19 | 1.7701 | -0.0017 | 0.0002 | 1.0000 | 1.8265 | 0.9991 |
| 0.20 | 1.8292 | -0.0019 | 0.0003 | 1.0000 | 1.8905 | 0.9990 |
| 0.21 | 1.8909 | -0.0022 | 0.0003 | 1.0000 | 1.9572 | 0.9989 |
| 0.22 | 1.9554 | -0.0025 | 0.0004 | 1.0000 | 2.0267 | 0.9988 |
| 0.23 | 2.0226 | -0.0029 | 0.0004 | 1.0000 | 2.0991 | 0.9987 |
| 0.24 | 2.0685 | -0.0031 | 0.0005 | 1.0000 | 2.1482 | 0.9987 |
| 0.26 | 2.1932 | -0.0038 | 0.0006 | 1.0000 | 2.2817 | 0.9985 |
| 0.28 | 2.3448 | -0.0047 | 0.0008 | 1.0000 | 2.4467 | 0.9984 |
| 0.30 | 2.4908 | -0.0057 | 0.0010 | 1.0000 | 2.5985 | 0.9983 |
| B. $-0.5, 0, 0.5$ -cm probe configuration | | | | | | |
| 0.17 | 1.6821 | -0.0015 | 0.0002 | 1.0000 | 1.7283 | 0.9993 |
| 0.18 | 1.7304 | -0.0013 | 0.0002 | 1.0000 | 1.7853 | 0.9992 |
| 0.19 | 1.7961 | -0.0016 | 0.0002 | 1.0000 | 1.8568 | 0.9991 |
| 0.20 | 1.8558 | -0.0018 | 0.0003 | 1.0000 | 1.9216 | 0.9990 |
| 0.21 | 1.9181 | -0.0021 | 0.0003 | 1.0000 | 1.9891 | 0.9989 |
| 0.22 | 1.9831 | -0.0024 | 0.0004 | 1.0000 | 2.0594 | 0.9988 |
| 0.23 | 2.0509 | -0.0028 | 0.0004 | 1.0000 | 2.1326 | 0.9987 |
| 0.24 | 2.0973 | -0.0030 | 0.0005 | 1.0000 | 2.1825 | 0.9986 |
| 0.26 | 2.2231 | -0.0037 | 0.0006 | 1.0000 | 2.3176 | 0.9985 |
| 0.28 | 2.3760 | -0.0046 | 0.0008 | 1.0000 | 2.4813 | 0.9983 |
| 0.30 | 2.5232 | -0.0055 | 0.0010 | 1.0000 | 2.6383 | 0.9982 |

higher than actual water loss measured gravimetrically (Figure 4), but slightly lower than gravimetric water loss during times of rapid transpiration. However, mean values agreed closely for the majority of measurements (Figures 5A and 5B).

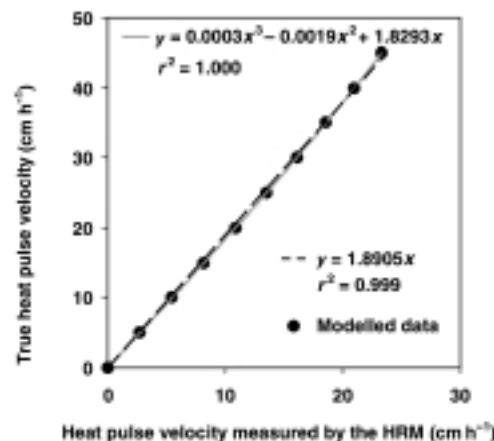


Figure 3. Comparison of a polynomial (shaded line) and linear (solid line) solution describing the modeled relationship between true heat pulse velocity and the smaller value that would be measured by the HRM due to wounding (filled circles). These data were generated for a $-0.6, 0, 0.6$ cm probe configuration (1.3-mm diameter, stainless steel probes) and a 0.20-cm wound width.

Discussion

Determining thermal diffusivity

Calculation of k by simultaneous solution with data from two heat pulse methods yielded plausible results. However, the simultaneous solution method is limited to cases where a second technique can be used with the HRM. Furthermore, even when probe sets for the different methods are installed adjacent to one another, radial and circumferential variations in sap flow are likely to hinder accurate comparisons between techniques.

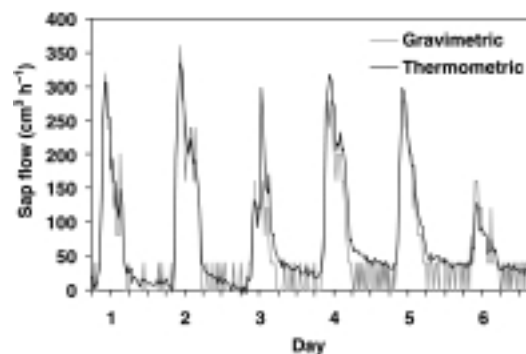


Figure 4. Comparison of gravimetric measurements of transpiration in a potted *E. marginata* tree with HRM measurements made on the same tree. (Note: disturbance to measurements near noon on Day 3 resulted from installation of an additional probe set.)

Values of k obtained empirically agreed well with results from the simultaneous solution method and had the advantage of requiring only measurements of water content and density of wood. Although further verification of the k values obtained with this method are required, we note that we successfully used these values in our validation experiments (Figures 4 and 5).

Hogg et al. (1997) used a method similar to the HRM that calculated thermal conductivity but did not convert this to thermal diffusivity for use with Equation 2. Because $K = k\rho c$ and ρc is equivalent to $\rho_b(c_w + m_c c_s)$ (the numerator of Equation 7), Hogg et al. (1997) retained K and combined the denominator of Equation 7 with Equation 2. Consequently, V_s was calculated directly, omitting calculation of V_h . Although this approach seems appealing, we did not adopt it for two reasons. First, Edwards et al. (1996) cautioned that polynomial solutions to wound effects (Swanson and Whitfield 1981) apply to V_h , but not to V_s or other derivatives of V_h , and hence heat pulse velocity must be calculated. Fortunately, linear approximations of the polynomial solution as used by Hogg et al. (1997) apply equally to V_h , V_s or Q . Second, we required calculations of V_h from the HRM for comparison with V_h values ob-

tained with the CHPM. Also, we required values of k for comparison with k values measured by other means.

Correction for wounding

Our numerical model indicated that wounding caused measured V_h to depart from actual V_h in an essentially linear function. Although the wound function is slightly sigmoidal, the r^2 values in Table 1A and the graphical comparison in Figure 3 suggest that a linear approximation describes the function with sufficient accuracy for small wound sizes. Interestingly, Hogg et al. (1997) generated coefficients for a $-0.75, 0, 0.75$ configuration based on a model similar to our HRM and corrected V_s by multiplying by a factor of 2.0 for a wound width of 2.0–2.2 mm, which is similar to the value of our B coefficient for a 2.0-mm wound (see Table 1).

Temperature effects

The finding that ambient temperature fluctuations caused V_h to fluctuate $0.5\text{--}1\text{ cm h}^{-1}$, with measurements closest to the root surface being most affected, suggests that the probes should be shielded from incident radiation. Generally, however, our observations indicated that ambient temperature fluctuations did not cause important or systematic measurement errors. During normal operation, the relatively large temperature changes caused by the heater ($1\text{--}2\text{ }^{\circ}\text{C}$) have a much greater influence on temperature ratios than the small fluctuations in ambient temperature. However, this finding argues for the use of the most powerful heating element that does not damage the plant.

Sensitivity to spacing

The relative importance of heat arising from the heating element as opposed to environmental heat inputs has a bearing on the choice of probe spacing as well as the design of the heater element. In this study, the widest probe spacing was the least reliable. Clearly, the further a temperature sensor is from the heating source, the less sensitive it will be to heat released by the heater.

Aside from temperature sensitivity, Marshall's (1958) statement that Equation 2 is only useful for v_1/v_2 ratios up to 20 is pertinent to the choice of probe spacing. Heat pulse velocities corresponding to v_1/v_2 ratios are shown for a range of probe spacings in Table 2. Narrower spacings appear capable of measuring high velocities, but are presumably less sensitive at low velocities because temperature ratios for a given velocity would be attenuated. Where probe design permits, the $-0.5, 0, 0.5$ cm spacing may be the most suitable if velocities are high.

Validation

The two validation experiments indicated that the HRM yields accurate measures of sap flow once probe bias, thermal diffusivity and wound effects have been corrected, radial and circumferential variation in rates of sap flow accounted for, and sap velocity calculated on an areal basis and then multiplied by the area of sapwood. The small overestimation of water loss during periods of minimum sap flow at night and the corresponding underestimation of water loss during periods of maximum transpiration might be expected if tissue water defi-

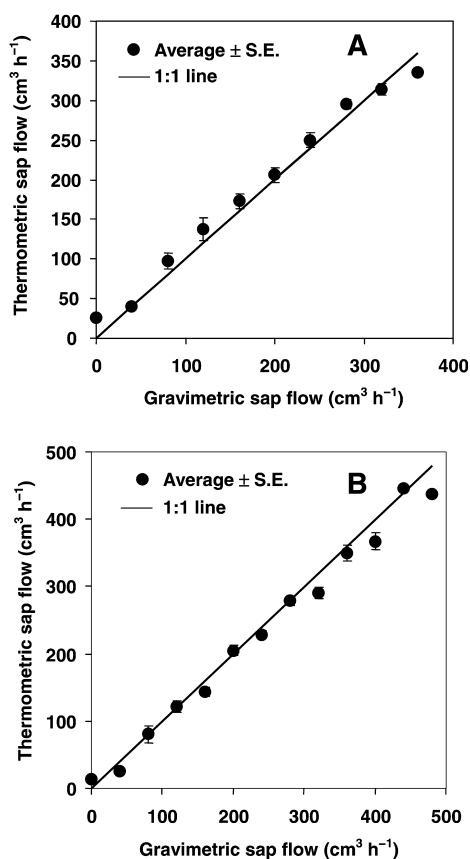


Figure 5. Relationship between gravimetric and thermometric measurements of transpiration in a potted *Eucalyptus marginata* tree based on (A) a $-0.6, 0, 0.6$ cm probe configuration and (B) a $-0.5, 0, 0.5$ cm probe configuration. The slightly sigmoidal function may be a result of capacitance. See also Burgess et al. (2000a) for an earlier data set from this series of experiments.

cits developed during the day and were reversed during the night.

General comparison of the HRM and CHPM

Comparative studies of measurements of V_h and Q made with the HRM and CHPM have been reported previously (Burgess et al. 1998, 2000b). Here we briefly compare the theoretical and practical limitations and advantages of each technique.

Range The range of heat pulse velocities that can be measured with the CHPM is about +4 (Becker 1998) to +60 cm h⁻¹ (Swanson 1983), with higher rates possible for altered spacings such as those used by Green and Clothier (1988). Assuming that Marshall (1958) is correct in stating that the maximum ratio of temperatures that can be measured accurately by symmetrically spaced heat pulse configurations is 20, the velocity range for an HRM configuration of -0.5, 0, 0.5 cm would be from -54 to +54 cm h⁻¹. Interestingly however, Swanson (1983) suggested that a -0.96, 0, 0.96 cm configuration could measure rates as high as 60 cm h⁻¹ (equating to temperature ratios of about 600). Gravimetric validation of HRM in trees growing with ample water in full sunlight and moderate temperatures is needed to test Swanson's claim and possibly extend the tested range of the HRM.

Sources of error and reliability

Both HRM and CHPM are sensitive to errors in probe placement. With the HRM, placement errors can be tested *in situ* and mathematically corrected, with more accuracy than methods that use physical means to determine probe positions. The CHPM is also sensitive to errors in measurement time, whereas the HRM is not as dependent on this parameter, although modeled wound corrections must take into account the measurement time used. The HRM requires the additional parameter of thermal diffusivity, which can be calculated in conjunction with wood water content and density.

Our general observation (based on some few million measurements made with the CHPM and HRM, Burgess et al. 1998, 2000b) is that data collected with the HRM are less prone to unexplained variation than their CHPM equivalents, at least with the equipment used. The probable cause of this improvement is that temperature ratios can be sampled several times and averaged during a given HRM measurement, whereas CHPM measurements rely on the single intersection of two (sometimes raggedly) converging probe temperatures. As suggested by T.J. Hatton (cited by Becker 1998), the use of curve fitting routines to estimate the time when probe temper-

atures converge may overcome this limitation of the CHPM.

Conclusions

The HRM provided accurate measurements of sap flow in xylem of woody plants that were comparable with those made with the CHPM (data not shown, but see Burgess et al. 2000b) over their common range, and included successful measurements over an augmented range unique to the HRM (low and reverse rates of flow, e.g., Figure 2).

The ability to measure low rates of sap flow is important for studies of whole-plant water use. Accurate measures of water use during the night, or other periods when transpiration rates are low, are critical to studies of water balance in dry, or seasonally dry environments. Similarly, the ability to measure low and reverse rates of flow accurately is critical to studies of hydraulic lift and hydraulic redistribution and their ecological significance to understory plants, as well as to studies of root water uptake under dry conditions.

The HRM technique has the potential to provide improved measurements of single plant transpiration and consequently stand transpiration and catchment water balance. In addition, studies of stem water storage, hydraulic architecture and hydraulic redistribution of water by root systems are likely to benefit by improvements to the scale at which measurements of sap flow can be made.

Acknowledgments

This work was supported by the Australian Centre for International Agricultural Research and the Australian Research Council. Support for S.S.O.B. was provided by the Western Australian Department of Conservation and Land Management. We thank Mark Bush, David Arthur, John Pate and Judy Eastham (UWA), Tom Hatton and Frank Dunin (CSIRO), Brett Ward (Agriculture Dept. Western Australia) and support staff from ICRAF.

References

- Barker, M. and P. Becker. 1995. Sap flow rate and sap nutrient content of a tropical rain forest canopy species, *Dryobalanops aromatica*, in Brunei. Selbyana 16:201–211.
- Barrett, D.J., T.J. Hatton, J.E. Ash and M.C. Ball. 1995. Evaluation of the heat pulse velocity technique for measurement of sap flow in rainforest and eucalypt forest species of south-eastern Australia. Plant Cell Environ. 18:463–469.
- Becker, P. 1996. Sap flow in Bornean heath and dipterocarp forest trees during wet and dry periods. Tree Physiol. 16:295–299.
- Becker, P. 1998. Limitations of a compensation heat pulse velocity system at low sap flow: implications for measurements at night and in shaded trees. Tree Physiol. 18:177–184.
- Becker, P. and W.R.N. Edwards. 1999. Corrected heat capacity of wood for sap flow calculations. Tree Physiol. 19:767–768.
- Benyon, R.G. 1999. Nighttime water use in an irrigated *Eucalyptus grandis* plantation. Tree Physiol. 19:853–859.
- Burgess, S.S.O., M.A. Adams and T.M. Bleby. 2000a. Measurement of sap flow in roots of woody plants: a commentary. Tree Physiol. 20:909–913.
- Burgess, S.S.O., J.S. Pate, M.A. Adams and T.E. Dawson. 2000b. Seasonal water acquisition and redistribution in the Australian woody phreatophyte, *Banksia prionotes*. Ann. Bot. 85:215–224.

Table 2. Effect of probe spacing on maximum velocities measured by HRM.

| Spacing (cm) | Maximum velocity (cm h ⁻¹) |
|--------------|--|
| 1.2 | 22.5 |
| 0.75 | 36 |
| 0.6 | 45 |
| 0.5 | 54 |

- Burgess, S.S.O., M.A. Adams, N.C. Turner and C.K. Ong. 1998. The redistribution of soil water by tree root systems. *Oecologia* 115:306–311.
- Cabibel, B. 1991. Thermal measurement of sap flow and hydric behavior in trees III. Influence on sap flow of trickle irrigation in cracked soil. *Agronomie* 11:877–888.
- Cohen, Y., S. Takeuchi, J. Nozaka and T. Yano. 1993. Accuracy of sap flow measurement using heat balance and heat pulse methods. *Agron. J.* 85:1080–1086.
- Dawson, T.E. 1996. Determining water use by trees and forests from isotopic, energy balance and transpiration analyses—the roles of tree size and hydraulic lift. *Tree Physiol.* 16:263–272.
- Dunlap, F. 1912. The specific heat of wood. USDA Forest Service Bulletin No. 110., 28 p.
- Dunn, G.M. and D.J. Connor. 1993. An analysis of sap flow in mountain ash (*Eucalyptus regnans*) forests of different age. *Tree Physiol.* 13:321–336.
- Dye, P.J. 1996. Response of *Eucalyptus grandis* trees to soil water deficits. *Tree Physiol.* 16:233–238.
- Dye, P.J. and B.W. Olbrich. 1993. Estimating transpiration from 6-year-old *Eucalyptus grandis* trees development of a canopy conductance model and comparison with independent sap flux measurements. *Plant Cell Environ.* 16:45–53.
- Dye, P.J., S. Soko and A.G. Poulter. 1996. Evaluation of the heat pulse velocity method for measuring sap flow in *Pinus patula*. *J. Exp. Bot.* 47:975–981.
- Edwards, W.R.N., P. Becker and J. Čermák. 1996. A unified nomenclature for sap flow measurements. *Tree Physiol.* 17:65–67.
- Edwards, W.R.N. and N.W.M. Warwick. 1984. Transpiration from a kiwifruit vine as estimated by the heat pulse technique and the Penman-Monteith equation. *N.Z. J. Ag. Res.* 27:537–543.
- Fenyvesi, A., C. Beres, A. Raschi, R. Tognetti, H.W. Ridder, T. Molnar, J. Rofler, T. Lakatos and I. Csiha. 1998. Sap-flow velocities and distribution of wet-wood in trunks of healthy and unhealthy *Quercus robur*, *Quercus petraea* and *Quercus cerris* oak trees in hungary. *Chemosphere* 36:931–936.
- Goldstein, G., J.L. Andrade, F.C. Meinzer, N.M. Holbrook, J. Cavelier, P. Jackson and A. Celis. 1998. Stem water storage and diurnal patterns of water use in tropical forest canopy trees. *Plant Cell Environ.* 21:397–406.
- Green, S.R. and B.E. Clothier. 1988. Water use of kiwifruit vines and apple trees by the heat-pulse technique. *J. Exp. Bot.* 39:115–123.
- Green, S.R. and B.E. Clothier. 1995. Root water uptake by kiwifruit vines following partial wetting of the root zone. *Plant Soil* 173:317–328.
- Green, S.R., B.E. Clothier and D.J. McLeod. 1997. The response of sap flow in apple roots to localised irrigation. *Agric. Water Manage.* 33:63–78.
- Hatton, T.J., S.J. Moore and P.H. Reece. 1995. Estimating stand transpiration in a *Eucalyptus populnea* woodland with the heat pulse method: Measurement errors and sampling strategies. *Tree Physiol.* 15:219–227.
- Hogg, E.H., T.A. Black, G. Denhartog et al. 1997. A comparison of sap flow and eddy fluxes of water vapor from a boreal deciduous forest. *J. Geophys. Res.* 102:28,929–28,937.
- Lassoie, J.P., D.R.M. Scott and L.J. Fritschen. 1977. Transpiration studies in Douglas-fir using the heat pulse technique. *For. Sci.* 23:377–390.
- Lide, D.R. 1992. Handbook of chemistry and physics, 73rd Edn. CRC Press Inc., Boca Raton, FL., pp 6–10.
- Lott, J.E., A.A.H. Khan, C.K. Ong and C.R. Black. 1996. Sap flow measurements of lateral tree roots in agroforestry systems. *Tree Physiol.* 16:995–1001.
- Marshall, D.C. 1958. Measurement of sap flow in conifers by heat transport. *Plant Physiol.* 33:385–396.
- McAneney, K.J., P.T. Prendergast, M.J. Judd and A.E. Green. 1992. Observations of equilibrium evaporation from a windbreak-sheltered kiwifruit orchard. *Agric. For. Meteorol.* 57:253–264.
- Moreno, F., J.E. Fernandez, B.E. Clothier and S.R. Green. 1996. Transpiration and root water uptake by olive trees. *Plant Soil* 184:85–96.
- Renquist, A.R., H.W. Caspari, M.H. Behboudian and D.J. Chalmers. 1994. Stomatal conductance of lysimeter-grown Asian pear trees before and during soil moisture deficits. *J. Am. Soc. Hort. Sci.* 119:1261–1264.
- Salama, R.B., G.A. Bartle and P. Farrington. 1994. Water use of plantation *Eucalyptus camaldulensis* estimated by groundwater hydrograph separation techniques and heat pulse method. *J. Hydrol.* 156:163–180.
- Smith, D.M. and S.J. Allen. 1996. Measurement of sap flow in plant stems. *J. Exp. Bot.* 47:1833–1844.
- Smith, D.M., N.A. Jackson, J.M. Roberts and C.K. Ong. 1999. Reverse flow of sap in tree roots and downward siphoning of water by *Grevillea robusta*. *Funct. Ecol.* 13:256–264.
- Swanson, R.H. 1983. Numerical and experimental analyses of implanted-probe heat pulse velocity theory. Ph.D. Thesis, University of Alberta, Edmonton, Canada, 298 p.
- Swanson, R.H. 1994. Significant historical developments in thermal methods for measuring sap flow in trees. *Agric. For. Meteorol.* 72:113–132.
- Swanson, R.H. and D.W.A. Whitfield. 1981. A numerical analysis of heat pulse velocity and theory. *J. Exp. Bot.* 32:221–239.
- Vertessy, R.A., T.J. Hatton, P. Reece, S.K. O'Sullivan and R.G. Benyon. 1997. Estimating stand water use of large mountain ash trees and validation of the sap flow measurement technique. *Tree Physiol.* 17:747–756.
- Wullschlegel, S.D., F.C. Meinzer and R.A. Vertessy. 1998. A review of whole-plant water use studies in trees. *Tree Physiol.* 18: 499–512.
- Zotz, G., S. Patino and M.T. Tyree. 1997. Water relations and hydraulic architecture of woody hemiepiphytes. *J. Exp. Bot.* 48: 1825–1833.

Copyright of Tree Physiology is the property of Oxford University Press / UK and its content may not be copied or emailed to multiple sites or posted to a listserv without the copyright holder's express written permission. However, users may print, download, or email articles for individual use.